Graphical Abstract

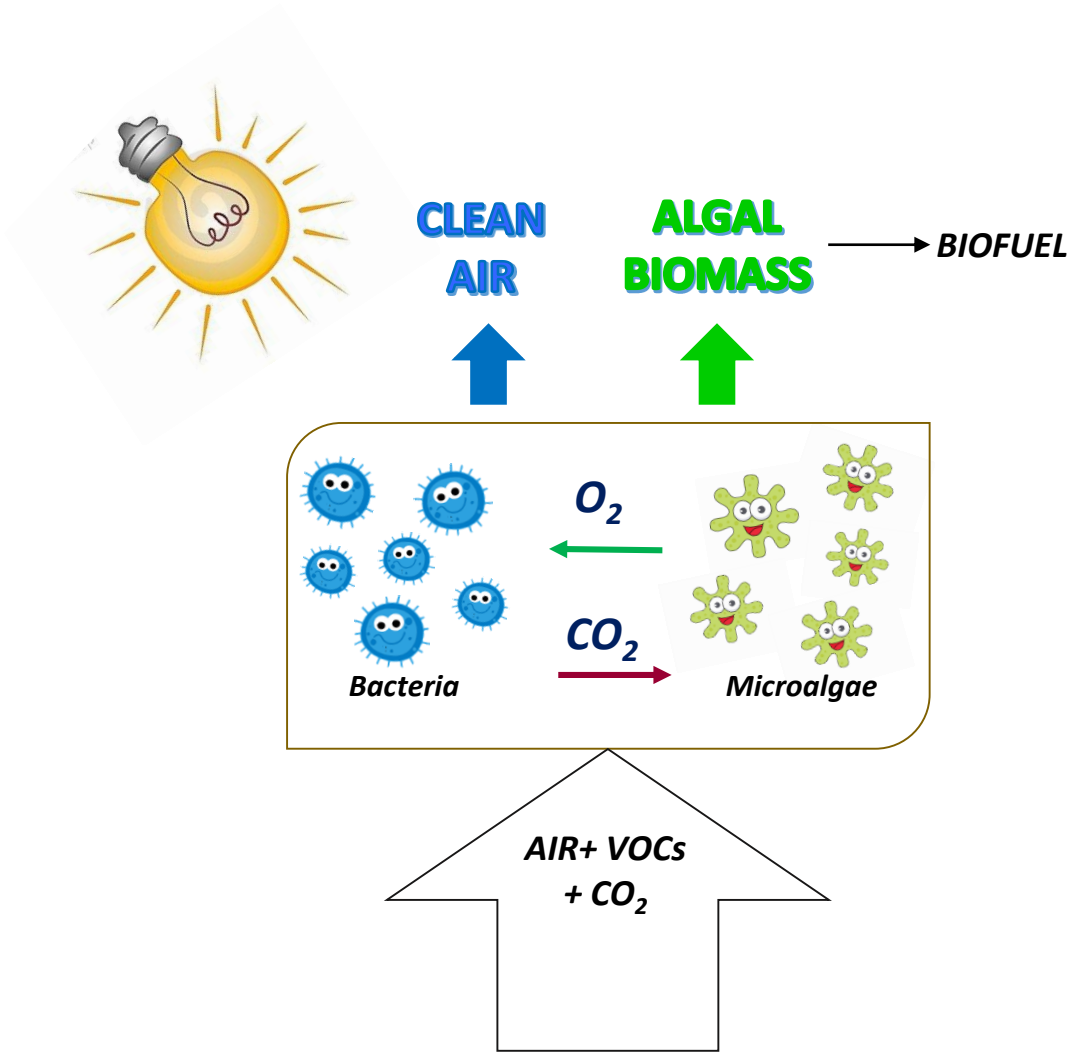

Comparative evaluation of a biotrickling filter and a tubular photobioreactor for the continuous abatement of toluene

Giuseppina Oliva[1,2], Roxana Ángeles[1,3], Elisa Rodríguez[1,3], Sara Turiel[4], Vincenzo Naddeo[2], Tiziano Zarra[2], Vincenzo Belgiorno[2], Raúl Muñoz[1,3], Raquel Lebrero[1,3*]

[1] Department of Chemical Engineering and Environmental Technology, University of Valladolid, Dr. Mergelina s/n., Valladolid 47011, Spain.

[2] SEED - Sanitary Environmental Engineering Division, Department of Civil Engineering, University of Salerno, via Giovanni Paolo II, Fisciano, SA, Italy

[3] Institute of Sustainable Processes, University of Valladolid, Dr. Mergelina s/n., Valladolid 47011, Spain.

[4] Department of Biodiversity and Environmental Management, University of León, 24071 León, Spain

[*]Author for correspondence: raquel.lebrero@iq.uva.es

Highlights

- Toluene removal efficiencies up to 96 % were achieved in both bioreactors
- BTF was more sensitive towards toxic metabolites due to a lower buffer capacity
- Microalgae activity resulted in high DO concentrations and CO_2 fixation
- TPBR exhibited higher process robustness towards process fluctuations than BTF

Abstract

The negative effects of volatile organic compounds (VOCs) on humans' health and the environment have boosted the enforcement of regulations, resulting in the need of effective and environmentally friendly off-gas treatment technologies. In this work, the synergism between microalgae and bacteria was investigated as a sustainable platform to enhance the biological degradation of toluene, herein selected as a model VOC. An innovative algal-bacterial tubular photobioreactor (TPBR) was systematically compared with a conventional biotrickling filter (BTF). Elimination capacities up to 24.8 g $m^{-3}h^{-1}$ were obtained in the TPBR, with removals up to 97%. Microalgae activity ensured high dissolved oxygen concentrations (~7.3 mgO_2 L^{-1}) and a reduced CO_2 emission. The conventional BTF supported average removal efficiencies of 84±16%, close to those obtained in the

TPBR (87±8%). However, the BTF was more sensitive towards the accumulation of secondary metabolites. In this regard, photosynthetic O_2 supplementation and CO_2 consumption by microalgae (which reduced the impact of acidification) enhanced process stability. The synergism between microalgae and bacteria represents an effective platform to ensure an enhanced VOC abatement performance, with reduced CO_2 emissions and the concomitant production of a valuable biomass.

Keywords: Algal-bacterial symbiosis; Biotrickling filter; Carbon dioxide fixation; Photobioreactor; Toluene abatement.

1. Introduction

In the last decades, atmospheric pollution has become an increasingly alarming problem due to its adverse effects at a global, regional and local scale, resulting in global warming, stratospheric O_3 depletion, ground level O_3 formation or acid rain among others [1–3]. In this context, the emissions of volatile organic compounds (VOCs) and odors from chemical manufacturing plants, petrochemical industry and other industrial sources pose a major challenge due to their detrimental effects on the environment and human health [4,5]. VOCs are included among the priority gas organic compounds, with BTEX (benzene, toluene, ethylbenzene and xylene) ranking 78 from 275 substances identified as the most dangerous for human health [6,7]. Furthermore, the volatile nature of VOCs often leads to odor-related complaints [1,8]. In particular, the toxicity and carcinogenicity of toluene to human health has triggered the enforcement of regulations, claiming for cost-effective and environmentally friendly technologies [9].

Physical-chemical technologies such as incineration, catalytic oxidation and adsorption represent widely used platforms for the removal of toluene [6,10]. However, their application for the abatement of industrial toluene-laden off-gases, typically characterized by high flow rates and relatively low VOCs concentrations (less than 100 ppm), is not economically feasible as a result of

their large consumptions of chemicals and energy [11,12]. Biological processes have become mature and low-cost alternatives to physical-chemical treatment technologies for VOCs degradation [10,13]. Biotrickling filters (BTFs) exhibit clear advantages over the rest of biotechnologies, including (i) better process stability and control of the operating parameters thanks to the continuous trickling of an aqueous nutrient solution, and (ii) reduced operating costs [5,14]. On the contrary, the treatment of high concentrations of VOCs in BTFs typically causes biomass overgrowth (packing media clogging), process inhibition due to acidification of the cultivation broth and a limitation of the oxygen available for the aerobic.

In this context, the synergisms between microalgae and bacteria in suspended-growth photobioreactors represent an efficient alternative to prevent O_2 limitation, acidification and biomass overgrowth operational problems during VOCs biodegradation. Microalgae produce oxygen during the photosynthetic process in the presence of light and CO_2, while heterotrophic bacteria utilize this additional O_2 supply to accelerate the oxidation of VOCs. In turn, the CO_2 resulting from VOC mineralization is photosynthetically fixed by microalgae with a concomitant rise in the pH of the cultivation medium. Furthermore, microalgal activity might not only prevent oxygen limitation but also enhance the biodegradability of the target VOC [11]. Despite their advantages, the number of studies exploring the merits of algal-bacterial photobioreactors for VOCs removal is scarce and a better understanding of the microbial communities and their interactions within the algal-bacterial consortia is necessary.

This work aims at evaluating and systematically comparing the continuous toluene abatement performance of a conventional bacterial BTF and an innovative tubular algal-bacterial photobioreactor (TPBR). The influence of the empty bed residence time (EBRT) and the toluene inlet concentration was investigated. Toluene mass transfer tests were carried out in order to determine the limiting stage under the operational conditions evaluated, and a final robustness test was performed to assess the capacity of the bioreactors to cope with toluene surges. The dynamics

of the microbial communities in both bioreactors were also determined using molecular biology techniques.

2. Materials and methods

2.1. Inoculum

Activated sludge from Valladolid wastewater treatment plant (Spain) was used as bacterial inoculum for both bioreactors. The inoculum of the BTF was prepared using 0.5 L of the activated sludge, centrifuged for 10 min at 10000 rpm and resuspended in 250 mL of fresh mineral salt medium (MSM) at a final total suspended solids (TSS) concentration of 5160 mg L^{-1}. The TPBR was inoculated with 0.5 L of the activated sludge (prepared as above described), and 1.2 L of microalgae culture (from a high rate algal pond (HRAP) operated in the Environmental Technology Group at University of Valladolid, Spain), centrifuged for 10 min at 10000 rpm and resuspended in 500 mL of fresh MSM at a final TSS concentration of 5940 mg L^{-1}.

2.2. Chemicals and mineral salt medium

The MSM used for BTF and TPBR operation was composed of (g L^{-1}): Na_2HPO_4 (2.44); KH_2PO_4 (1.52); NH_4SO_4 (1); $MgSO_4 \cdot 7H_2O$ (0.2) and $CaCl_2 \cdot 2H_2O$ (0.05) and 10 mL L^{-1} of SL-4 stock solution containing: EDTA (0.5 g L^{-1}) and $FeSO_4 \cdot 7H_2O$ (0.2 g L^{-1}) and 100 mL L^{-1} of SL-6 stock solution composed of (g L^{-1}) $ZnSO_4 \cdot 7H_2O$ (0.1); $MnCl_2 \cdot 4H_2O$ (0.03); H_3BO_3 (0.3); $CoCl_2$ (0.2); $CuCl_2 \cdot 2H_2O$ (0.01); $NiCl_2 \cdot 6H_2O$ (0.02); $Na_2MoO_4 \cdot 2H_2O$ (0.03). Toluene was purchased from PANREAC (Barcelona, Spain) with a purity of 99.8%.

2.3. Experimental set-up and operating procedureThe BTF consisted of a cylindrical jacketed

PVC column with an inner diameter of 0.08 m and a height of 0.79 m (Figure 1). The column was packed with plastic Kaldnes rings (Evolution Aqua, United Kingdom) at a working volume of 4 L. The recirculation of MSM was carried out by a peristaltic pump (Watson-Marlow 520S IP31) from an external 1.2 L jacketed holding tank stirred at 400 rpm (Agimatic-S, Selecta®, Spain). The MSM was continuously recycled counter-currently at a trickling liquid velocity (TLV) of 2 m h^{-1}. The synthetic toluene-laden emission was supplied from the bottom of the BTF.

The 45.6 L TPBR consisted of tubes with an internal diameter of 5 cm and a total length of 20 m. The TPBR was interconnected, via liquid recirculation, to a 2 L vertical absorption column (AC, height = 120 cm, inner diameter = 4.5 cm) and a 70 L mixing chamber (44 cm × 33 cm × 49 cm). The cultivation broth was recirculated through the TPBR tubes at a linear velocity of 0.53 m s^{-1}, while the liquid to gas flow rate ratio (L/G) in the AC was set at 0.5. Cool white LEDs were arranged vertically at both sides of the TBPR and configured with a 12:12 h:h light-dark illumination regime. The synthetic toluene-laden emission was supplied via a metallic diffuser (located at the bottom of the AC) co-currently with the algal-bacterial cultivation broth recirculated from the mixing chamber. The synthetic polluted stream was obtained by injecting pure liquid toluene at a specific flow rate directly into the inlet compressed air line by means of a syringe pump (Fusion 100, Chemyx Inc. USA). The resulting gas stream was divided into two streams using gas flow rotameters (Aalborg, USA) prior feeding the bioreactors.

The systems were operated for 90 days testing four different operating conditions, gradually increasing the inlet load (IL) (Table 1). The MSM renewal rate was subsequently increased to 400 (stages II-III), 800 (stage IVa) and 1600 mL d^{-1} (stages IVb-IVc). The pH of the fresh MSM daily exchanged in the BTF was manually adjusted at 8.5 (by addition of a NaOH solution 5 M) from day 74 onwards. No chemicals were added to control the pH in the TPBR. Finally, the light intensity in the TPBR was adjusted at ~50 µmol m^{-2} s^{-1} during the first 74 days and increased afterwards at ~150 µmol m^{-2} s^{-1}.

Inlet and outlet toluene, CO_2, N_2 and O_2 concentrations in the gas phase, and pH and dissolved oxygen (DO) in the cultivation broth of the bioreactors were daily analyzed. Liquid samples for the determination of the concentration of total organic carbon (TOC), total nitrogen (TN), nitrite and nitrate were taken three times per week. Samples of the inoculum and the cultivation broth at the end of each operating stage in the TPBR and of the inoculum and the biofilm at the end of the experimental period in the BTF were drawn to carry out a characterization of the microalgae and/or bacterial population structure.

Table 1 – Operating parameters during the different operational stages in the BTF and the TPBR

Stage	**I**	**II**	**III**	**IVa**	**IVb**	**IVc**
Days	0-13	14-37	38-58	58-69	70-74	75-83
IL_{BTF} (g m^{-3} h^{-1})	4.5	9	12	24	24	24
IL_{TPBR} (g m^{-3} h^{-1})	4.95	9.9	13.2	26.4	26.4	26.4
EBRT (min)	2	1	0.75	0.75	0.75	0.75
Q_{TPBR} (mL min^{-1})	1100	2200	2933	2933	2933	2933
Q_{BTF} (mL min^{-1})	2000	4000	5333	5333	5333	5333
Toluene inlet concentration (g m^{-3})	0.15	0.15	0.15	0.3	0.3	0.3
MSM renewal rate (mL d^{-1})	200	400	400	800	1600	1600
BTF pH control	No	No	No	No	No	Yes
TPBR light intensity (µmol m^{-2} s^{-1})	~50	~50	~50	~50	~50	~150

2.4 Mass transfer and robustness tests

A mass transfer test was performed under steady state condition in each operational stage in order to elucidate whether bioreactors performance was limited by mass transfer of toluene from the gas to the liquid phase or by microbial activity. For this purpose, inlet toluene concentration was increased by a factor of ~3 for 5 hours, hourly monitoring the inlet and outlet toluene and CO_2 gas concentrations. This increase in the inlet toluene concentration resulted in a higher gas-liquid concentration gradient and therefore in a proportional increase in the amount of toluene potentially transferred to the liquid phase according to the Fick's law (Equation 1):

$$F_i = K_L a \left(\frac{C_{i,G}}{H} - C_{i,L} \right)$$ Equation 1

where F_i is the volumetric toluene mass transfer rate (g m^{-3} h^{-1}), $K_L a$ is the overall volumetric mass transfer coefficient (h^{-1}), $C_{i,G}$ and $C_{i,L}$ are the toluene concentrations in the gas and liquid phases (g m^{-3}), respectively, and H is the Henry's Law constant.

A robustness test in both bioreactors was also carried out by the end of the experiment. Toluene feeding was switched off for 3 days in order to simulate typical operating conditions in a manufacturing plant (air extraction shutdown during the weekend). Inlet and outlet toluene and CO_2 gas concentrations and pH in the liquid media were measured hourly for the first 5 hours following toluene feed resumption, and then twice a day until stabilization.

2.5 Analytical methods

Toluene gas concentrations were analyzed in a Bruker 3900 gas chromatograph (Palo Alto, USA) equipped with a flame ionization detector and a Supelco Wax (15 m × 0.25 mm × 0.25 µm) capillary column. Oven temperature was initially maintained at 50 °C for 1 min, increased at 50 °C min^{-1} up to 70 °C and then at 65 °C min^{-1} to a final temperature of 140 °C. N_2 was used as the carrier gas at 1 mL min^{-1}. CO_2, N_2 and O_2 gas concentrations were determined in a Bruker 430 gas chromatograph (Palo Alto, USA) coupled with a thermal conductivity detector and equipped with a CP-Molsieve5A (15 m × 0.53 m × 15 m) and a P-PoraBOND Q (25 m × 0.53 m × 10 m) columns. The oven, injector and detector temperatures were maintained at 40, 150 and 175 °C, respectively. Helium was used as the carrier gas at 13.7 mL min^{-1}. Gas sample injections were carried out with a 100 µl gas-tight glass syringe (Hamilton, USA).

DO concentration in the culture broth of the TPBR was monitored by an OXI 330i oximeter (WTW, Germany). The pH of the liquid samples was determined by a Crison 50 12T pH meter (Crison Instruments, Spain). Biomass concentration was measured as TSS according to Standard Methods (American Water 167 Works Association, 2012). Samples for the determination of TOC

concentrations were filtered through 0.22 µm filters (Merck Millipore. USA) prior analysis in a TOC-VCSH analyzer (Shimadzu, Japan)..

2.6 DNA extraction, Illumina Library preparation and bioinformatic analysis

Biomass samples were drawn at different stages during the experimental period and stored at -20 ºC prior to sequencing microbial analysis: BTF_0_AS (activated sludge inoculum of the BTF), BTF_IV (end of operation of the BTF, stage IVc), TPBR_0_HRAP (microalgae inoculum of the TPBR), TPBR_0_MIX (activated sludge + microalgae inoculum of the TPBR), and TPBR_II, TPBR_III and TPBR_IV (end of stages II, III and IVc in the TPBR, respectively). DNA extraction was performed using the Fast DNA Spin kit for soil (MP Biomedicals, LLC) according to the manufacturer's instructions but optimizing the time for cell lysis and the time for optimal DNA binding to the silica matrix. DNA integrity was checked by agarose gel (1.2 % (w/v)) electrophoresis. DNA concentration was determined using a NanoDrop spectrophotometer (NanoDrop Technologies, 154 Wilmington, USA). The extracted DNA was stored at -20ºC prior to 16S rDNA amplicon sequencing analysis. An aliquot of 5 ng μL^{-1} of genomic DNA was used to initiate the library preparation protocol (16S rDNA gene Metagenomic Sequencing Library Preparation Illumina protocol). Primers for 16S rDNA amplification targeted gene V3 and V4 regions [15]. Illumina adapter overhang nucleotide sequences were added to the gene- specific sequences. After 16S rDNA gene amplification, the multiplexing step was performed using the Nextera XT DNA Library Preparation Kit (Illumina, San Diego, CA) with a reduced number of PCR cycles (25) using 55º C as annealing temperature. 1 µl of the PCR product was run on a Bioanalyzer DNA 1000 chip to verify the size (expected size ~550 bp). After size verification the libraries were sequenced using a 2 × 300pb paired-end run (MiSeq Reagent kit v3 (Illumina, San Diego, CA)) on a MiSeq Sequencer according to manufacturer's instructions (Illumina). Sequencing analysis was carried out by the Foundation for the Promotion of Health and Biomedical Research of Valencia Region (FISABIO, Spain).

Quality assessment of sequencing data was performed using the PRINSEQ-LITE program [16] applying the following parameters: minimum read length: 50, trimming quality right: 30; trimming quality type: mean; trimming quality window: 20. The sequence data was analyzed using qiime2 pipeline [17]. After quality assessment, denoising, paired-end reads joining, and chimera depletion was performed using DADA2 pipeline [18]. Taxonomic affiliations were assigned using the Naive Bayesian classifier integrated in quiime2 plugins using the SILVA_release_132 database [19]. Inverse Simpson (ID) and Shannon indexes (H) were calculated using the Vegan library version 2.3e1[20]. The Krona hierarchical browser tool [21] was used to represent relative abundances of the different taxa within the microbial communities in the analyzed samples. The 16S rRNA sequence data sets was deposited in the National Center for Biotechnology Information (NCBI) under the study (BioProject) PRJNA505981 (http://www.ncbi.nlm.nih.gov/bioproject/505981).

2.7 Microalgae identification

Samples for the analysis of microalgae population in the TPBR were withdrawn at the beginning of the experimental period and by the end of stages II, III and IVc, fixed with lugol acid at 5% and stored at 4 °C prior to analysis. The identification, quantification and biometry measurements of the microalgae assemblage at steady state were performed by microscopic examination (OLYMPUS IX70, USA).

3. Results and discussion

3.1. BTF performance

Toluene removal efficiency (RE) reached average values of 90 ± 3 % during stage I. This RE corresponded to steady state elimination capacities (ECs) of 4.1 ± 0.6 g $m^{-3}h^{-1}$ (**Error! Reference source not found.**) and CO_2 production rates (PCO_2) of 10.6 ± 3.9 g m^{-3} h^{-1} (**Error! Reference source not found.**). This PCO_2 was close to the theoretical CO_2 production ($ThPCO_2$), resulting in a toluene mineralization rate of ~71 %. The acidic metabolites resulting from microbial toluene biodegradation supported a decrease in the pH of the recycling media from 7.12 to 6.72 by day 13

(**Error! Reference source not found.**S1). A toluene mass transfer test was carried out at the end of stage I (Figure S2). During the test, a ~3 times higher EC was recorded in the BTF when increasing the toluene IL, suggesting that the process was limited by toluene mass transfer from the gas to the liquid phase. In the stage II, the EBRT was reduced from 2 to 1 min; a drop in the RE to 61 % was observed by day 23 of operation, likely due to an accumulation of inhibitory intermediate metabolites as also observed in previous studies focused on the aerobic biodegradation of BTEX [22,23]. Nevertheless, the system rapidly recovered former toluene abatement performance, reaching a stable EC of 7.49 ± 1.08 g $m^{-3}h^{-1}$ from day 27 onwards. A mass transfer test was also conducted in stage II: the increase in the EC during up to a maximum EC of 23.22 g $m^{-3}h^{-1}$ demonstrated that the system was limited by toluene mass transfer (Figure S3). During stage III, an EBRT of 45 seconds and an inlet toluene concentration of 150 mg m^{-3} were set. The increase in IL also resulted in a higher PCO_2 of 52.8 ± 8.9 g of CO_2 $m^{-3}h^{-1}$ that exceeded the theoretical CO_2 production . This result was attributed to an active endogenous respiration of the bacterial community [10,24]. Gas-liquid mass transfer was also confirmed as the limiting factor also in this stage III (Figure S4). During stage IV, the inlet concentration was doubled to 300 mg m^{-3};the BTF initially supported a RE of 89 ± 7% from day 59 to 66. However, a sharp drop in the toluene abatement performance was observed by day 69, when the RE decreased to 52%. This decrease in toluene degradation resulted in a concomitant reduction in CO_2 production, and was attributed to the acidification of the system. The progressive decrease in pH observed during this stage IVa (Figure S1), which likely inhibited microbial activity, confirmed this hypothesis [25].

In this context, the MSM renewal rate was increased by a factor of 2 (Stage IVb) in order to remove the toxic metabolites accumulated in the recycling medium. The increase in MSM renewal resulted in the rapid recovery of the RE and the concomitant increase in PCO_2. However, a gradual decrease in the pH was again recorded from day 74 onwards, thus it was manually adjusted by increasing the pH of the fresh MSM up to 8.5 via NaOH addition in order to prevent a new reduction in the

toluene EC (Stage IVc). During this last stage, the PCO_2 was slightly lower than the $ThPCO_2$ and the RE averaged 84 ± 15%. The last mass transfer test revealed that despite the performance of the BTF was still limited by gas-liquid mass transfer, a lower EC increase was observed when increasing the IL (EC = 45.9 ± 2.8 g $m^{-3}h^{-1}$ at an IL of 72.7 ± 4.9 g $m^{-3}h^{-1}$).

3.2. TPBR performance

The TPBR rapidly achieved an average removal efficiency of 88 ± 3% during stage I, corresponding to an EC of 3.82 ± 0.94 g $m^{-3}h^{-1}$ (at an IL = 4.59 ± 0.57 g m^{-3} h^{-1}) (**Error! Reference source not found.**). Despite the fact that the TPBR supported an effective toluene degradation activity, the outlet CO_2 gas concentrations were lower than the inlet concentrations as a result of microalgae photosynthetic CO_2 fixation (**Error! Reference source not found.**). Indeed, a significant fraction of the CO_2 produced during pollutant mineralization in algal-bacterial systems is fixed by microalgae. Moreover, algal photosynthesis also ensured a high DO concentration in the cultivation medium [26], which averaged 7.73 ± 0.94 mgO_2 L^{-1}. A mass transfer test was performed by increasing the toluene IL up to 11.13 ± 0.68 g $m^{-3}h^{-1}$ corresponding to an increase in EC up to 9.93 ± 0.62 g $m^{-3}h^{-1}$.In stage II, the IL entering the TPBR was doubled , which resulted in an average RE of 87 ± 5%. CO_2 production rates increased concomitantly with the increase in toluene EC. Thus, a PCO_2 value of 17.56 ± 6.72 g m^{-3} h^{-1} (corresponding to almost half of the $ThPCO_2$) was observed (Figure 5). The mass transfer test carried out in stage II revealed that toluene mass transport from the gas to the liquid phase was the limiting step (Figure S3). A further increase in the IL during stage III lead to an increase in the EC up to 12.79 ± 3.08 g $m^{-3}h^{-1}$ (Figure 4). A stable toluene removal was also recorded in this stage (RE = 89 ± 3%), where CO_2 production remained lower than the theoretical value (PCO_2 = 18.77 ± 12.53 g $m^{-3}h^{-1}$ *vs.* $ThPCO_2$ = 48.46 ± 11.82 g $m^{-3}h^{-1}$). No significant variations in the pH or the TSS concentrations were observed during stages II and III (average values of pH = 6.03 ± 0.8 and TSS = 119 ± 29 mg L^{-1}). The mass transfer test in stage

III confirmed process limitation by toluene mass transfer (Figure S4). Finally, when IL in stage IV was set at 23.42 ± 1.39 g $m^{-3}h^{-1}$, the TPBR supported an EC of 20.93± 1.50 g $m^{-3}h^{-1}$. Interestingly, the increase in IL did not trigger a decrease in toluene RE, which remained stable at 89 ± 3%. It is worth noting that a higher biomass production was however recorded during stage IV, resulting in an increase in the algal biomass concentration (measured as TSS) from 170 to 410 mg L^{-1} from day 58 to 90. The higher algal biomass concentration promoted the reduction in the net PCO_2 because of the enhanced photosynthetic activity [27]. A progressive decrease in the pH of the TPBR cultivation broth was recorded from day 68 onwards. Despite no detrimental effect on process performance had been observed, the light intensity was increased to 148.31 µmol m^{-2} s^{-1} in order to increase the pH of the cultivation mediated by photosynthetic CO_2 uptake (Stage IVc). The higher light intensity resulted in a trend reversal in the pH [28]. The mass transfer test carried out by the end of the experiment highlighted that the system was also limited by mass transfer under the conditions implemented during stage IV (Figure S5).

3.3. Robustness test

A robustness test was performed by the end of the experiment to evaluate the capacity of both bioreactors to cope with fluctuations in the IL (Figure S6). To this end, the toluene-loaded air feeding system was stopped for 3 days, while maintaining the mineral medium recirculation. The TPBR recovered the removal capacity immediately after the restoration of the polluted air supply, achieving a RE of 93 ± 3%. On the contrary, the BTF did not achieve previous steady state removal efficiencies. Indeed, a RE of 77 ± 5% was recorded nine hours after toluene feeding resumption, which was significantly lower than the removals recorded during stage IVc (86 ± 12%). Overall, the TPBR exhibited a higher process robustness towards process fluctuations than the BTF.

3.4. Comparative evaluation

The initial RE of 30 % recorded in the TPBR following the start-up of both reactors was attributed to the higher absorption capacity of the photobioreactor cultivation broth. During stage I, the bioreactors showed comparable performances. However, the presence of the algal-bacterial

consortium in the TPBR resulted in an increase in DO and the simultaneous CO_2 fixation. For this reason, the TPBR rapidly showed CO_2 outlet concentrations significantly lower than those recorded in the BTF outlet. The BTF was also more sensitive towards the presence of secondary inhibitory metabolites due to the lower liquid volume and thus lower buffer capacity. Indeed, the build-up of metabolites may trigger process instability due to their mutagenic effects on the culture [29]. As previously observed by Bordel et al. [30], the generation of secondary metabolites can be induced by a toluene overload or a limiting O_2 concentration in the aqueous phase. In this context, the TPBR exhibited a higher adaptability to inlet load fluctuations both because of the larger amount of liquid involved and of the higher DO concentrations in the cultivation broth. CO_2 consumption by microalgae also enhanced process stability by reducing the acidification effects. Finally, the mass transfer tests pointed out that, regardless of the operational conditions, both processes were limited by toluene mass transfer from the gas phase to the biofilm or to the liquid phase.and the PCO_2 remained stable, suggesting that pollutants accumulation did not occur and thus the toluene supplied was mineralized by the microbial community. However, when increasing the toluene inlet concentration, the TPBR supported an EC closer to the transient IL, which confirmed that the tubular photobioreactor responded better to higher toluene loads compared to the BTF.

3.5. Microbial community analysis

Read numbers after quality filtering and chimera filtering ranged between 77,059 (TPBR_0_MIX) and 34,891 (BTF_IV) (Table 2). The number of resulting OTUs varied between 874 (BTF_0_AS) and 101 (BTF_IV) (Table 2). The inoculum of the BTF showed significantly higher OTU number and H and ID index values than the biofilm sample retrieved in the BTF by the end of the experiment (BTF_IV). In this context, the simplification of the feed and the operating conditions applied mediated the reduction in the diversity of the microbial. Accordingly, the number of phyla detected in BTF_0 was 34, decreasing to 14 in BTF_IV. Interestingly, the OTU number and H and ID indexes corresponding to the inoculum of the TPBR were lower than those measured in the BTF_0_AS. This reduction was attributed to the enrichment of the most abundant species after the

mixture (i.e. *Proteobacteria*) while the representation of the less abundant species decreased and could not be detected. The operating conditions tested in the TPBR from stage II onwards resulted in a decrease in OTU richness compared to the inoculum, however H and ID indexes remained similar or even higher. From these data, it can be inferred that operating conditions mainly impacted the ID index, which mostly depends on the most abundant species, rather than the H index, which gives greater relevance to less abundant species. Therefore, the specialization of the microbial communities to toluene feeding was mainly associated to a richness loss in the TPBR rather than to an evenness loss [31,32].

Table 2. OTU richness and Shannon and Inverse Simpson diversity indices.

Sample ID	Non chimeric reads	OTUs (richness)	Shannon index	Inv. Simpson index
BTF_0_AS	69,767	874	2.16	5.46
BTF_IV	34,891	101	1.08	2.38
TPBR_0_HRAP	57,451	276	1.5	2.89
TPBR_0_MIX	77,059	582	1.66	3.3
TPBR_II	52,019	171	1.85	5.68
TPBR_III	70,405	174	1.39	2.92
TPBR_IV	59,261	104	1.36	3.01

Proteobacteria was the most abundant phylum during the operation of the reactors (BTF_IV: 55 %, TPBR_III: 52 %, TPBR_IV: 49 %), except in TPBR_II, which was dominated by a wider range of bacterial phyla (*Proteobacteria*: 20 %, *Cyanobacteria*: 20 %, *Actinobacteria*: 18 %, *Bacteroidetes*: 18 %, *Chlamydiae*: 17 %) (Figure 6a). Interestingly, *Actinobacteria* was more abundant in TPBR_II and BTF_IV samples, suggesting that toluene inlet concentration and the presence of photosynthetic organisms influenced its occurrence in the reactors. This finding agreed with previous studies that identified *Proteobacteria* as the dominant group in an algal-bacterial airlift photobioreactor and bacterial reactor treating toluene at high inlet loads (369-480 g m^{-3} h^{-1}) [11,33]. At lower toluene loads (0.5 - 14 g m^{-3} h^{-1}), *Actinobacteria* were mostly represented [33]. In this work,

Mycobacterium and *Rhodococcus* were dominant, both genera being able to grow at low toluene concentrations [34] (Figure S7).

Among *Proteobacteria, Gammaproteobacteria* was a highly abundant class in all samples (Figure 6b). This class now includes *Betaproteobacteria* class as an order: the *Betaproteobacteriales* [35], which is a highly abundant group in rhizospheric and freshwater environments [36–38], where they play important roles in nitrogen cycling [39] and are known to produce plant growth promoting substances such as phytohormones [40]. *Betaproteobacteriales* (*Burkholderiaceae*) and *Xanthomonadales* (*Rhodanobacteraceae*) were dominant among *Gammaproteobacteria* (Figure 7a and 7b). At the highest inlet load (stage IV), *Xanthomonadales* prevailed over *Betaproteobacteriales* in both the BTF and the TPBR (Figure 7a), highlighting their role at higher toluene concentrations. *Burkholderiales* have been identified as main toluene degraders (20 % of the entire bacterial community) in a constructed wetland; while most of the remaining bacterial community likely utilized other carbon sources derived from plant roots [37]. Similarly, bacteria in microalgal-bacterial consortium might utilize organic carbon released by microalgae, and in return, supply inorganic and low molecular weight organic carbon for algal growth, enhancing process stability in the TPBR [41]. . In fact, it has been observed that *Burkholderiales* maintained stable toluene turnover in a constructed wetland treating toluene by feeding on organic root exudates, while reutilizing the stored carbon compounds [42]. Many bacterial groups detected in the are able to grow in mutualistic association with several species of green algae [43,44] or even rely on an eukaryotic host for cell survival [45] as is the case of *Chlamydiae* (Figure 6a). This highlights the importance to unravel microalgae and bacteria interactions in algal-based photobioreactors to boost VOCs removal performance.

3.6. Microalgae population

Chlorella vulgaris and Chlorella minutissima were the dominant species in the inoculum of the TPBR (56 and 26 %, respectively) (Figure S8). These species were gradually replaced by

Scenedesmus obliquus, which was the dominant species during stage II. From this stage on, a gradual increase was observed the abundance of *Chlamydomonas sp*., among the top 8 genera of microalgae tolerant to organic pollution [46]. Unfortunately, no specific correlation between operating conditions and evolution of microalgae population was elucidated. Nevertheless, the evolution of microalgae population was likely linked to the evolution of bacterial communities, since it has been demonstrated that specific microalgae populations are associated with unique and specific microbial groups [43].

4. Conclusions

This work demonstrated the potential of the synergisms between bacteria and microalgae to support an effective and environmentally friendly toluene biodegradation. The high DO concentrations and higher pH values mediated by photosynthesis resulted in improved and more stable performances in the TPBR compared to the BTF. In this regard, average ECs of 13,58 ± 0,56 g $m^{-3}h^{-1}$ and REs of 88% ± 10% were achieved in the tubular photobioreactor. Consistently, several bacteria that grow in mutualistic association with green algae were detected in the TPBR. The BTF (dominated by *Proteobacteria* and *Actinobacteria* at the end of the experiment) supported similar toluene removal, but it suffered from performance deterioration mainly due to secondary metabolites accumulation and acidification of the recirculating medium, which inhibited microbial activity. Finally, CO_2 fixation by microalgae in the TPBR resulted in a reduction in CO_2 emissions and the production of a valuable biomass suitable for further revalorization. Overall, the synergism between microalgae and bacteria may be considered an effective solution for the simultaneous abetment of greenhouse gases and toluene.

Acknowledgements

This research was supported by the Regional Government of Castilla y León and the EU-FEDER project (UIC 71 and CLU-2017-09 project). The PhD School in "Risk and Sustainability in Civil Engineering, Environmental and Construction" and the "Erasmus Plus Programme" are also acknowledged for the mobility grant of G. Oliva.

Figure captions

Figure 1. Schematic representation of the experimental set-up. GSP: Gas sampling ports. LSP: Liquid sampling ports

Figure 2. Time course of the toluene inlet load (···×···), elimination capacity (—▲—) and removal efficiency (- - ■- -) in the biotrickling filter. Vertical lines separate different operating stages as indicated in the upper part of the graph.

Figure 3. Time course of the real CO_2 production (PCO_2 —▲—) and the theoretical CO_2 production ($ThPCO_2$ ···×···) in the biotrickling filter. Vertical lines separate different operating stages as indicated in the upper part of the graph.

Figure 4. Time course of the toluene inlet load (···×···), elimination capacity (—▲—) and removal efficiency (- - ■- -) in the tubular photobioreactor. Vertical lines separate different operating stages as indicated in the upper part of the graph.

Figure 5. Time course of the real CO_2 production (PCO_2 —▲—) and the theoretical CO_2 production ($ThPCO_2$ ···×···) in the photobioreactor.

Figure 6. Bacterial community composition of the inocula, BTF and TPBR at the phylum (a) and class (b) taxonomic ranks.

Figure 7. Bacterial community composition in the inocula, BTF and TPBR at the order (a) and family (b) taxonomic ranks.

Bibliography

[1] B.T. Mohammad, M.C. Veiga, C. Kennes, Mesophilic and thermophilic biotreatment of BTEX-polluted air in reactors, Biotechnol. Bioeng. 97 (2007) 1423–1438. doi:10.1002/bit.21350.

[2] J. Paca, E. Klapkova, M. Halecky, K. Jones, C.R. Soccol, Performance evaluation of a biotrickling filter degrading mixtures of hydrophobic and hydrophilic compounds, Clean Technol. Environ. Policy. 9 (2007) 69–74. doi:10.1007/s10098-006-0054-7.

[3] A.K. Mathur, C. Balomajumder, Biological treatment and modeling aspect of BTEX abatement process in a biofilter, Bioresour. Technol. 142 (2013) 9–17. doi:10.1016/j.biortech.2013.05.005.

[4] Y.-C. Hsu, S.-K. Chen, J.-H. Tsai, H.-L. Chiang, Determination of Volatile Organic Profiles and Photochemical Potentials from Chemical Manufacture Process Vents, J. Air Waste Manage. Assoc. 57 (2007) 698–704. doi:10.3155/1047-3289.57.6.698.

[5] S. Mudliar, B. Giri, K. Padoley, D. Satpute, R. Dixit, P. Bhatt, R. Pandey, A. Juwarkar, A. Vaidya, Bioreactors for treatment of VOCs and odours – A review, J. Environ. Manage. 91 (2010) 1039–1054. doi:10.1016/j.jenvman.2010.01.006.

[6] I. Akmirza, C. Pascual, A. Carvajal, R. Pérez, R. Muñoz, R. Lebrero, Anoxic biodegradation of BTEX in a biotrickling filter, Sci. Total Environ. 587–588 (2017) 457–465. doi:10.1016/j.scitotenv.2017.02.130.

[7] J.R. Robledo-Ortíz, D.E. Ramírez-Arreola, A.A. Pérez-Fonseca, C. Gómez, O. González-Reynoso, J. Ramos-Quirarte, R. González-Núñez, Benzene, toluene, and o-xylene degradation by free and immobilized P. putida F1 of postconsumer agave-fiber/polymer foamed composites, Int. Biodeterior. Biodegradation. 65 (2011) 539–546. doi:10.1016/j.ibiod.2010.12.011.

[8] T. Zarra, V. Naddeo, V. Belgiorno, Characterization of odours emitted by liquid waste treatment plants (LWTPs), Glob. Nest J. 18 (2016) 721–727.

[9] Z. Wang, G. Xiu, T. Qiao, K. Zhao, D. Zhang, Coupling ozone and hollow fibers membrane bioreactor for enhanced treatment of gaseous xylene mixture, Bioresour. Technol. 130 (2013) 52–58. doi:10.1016/j.biortech.2012.11.106.

[10] J.M. Chen, R.Y. Zhu, W.B. Yang, L.L. Zhang, Treatment of a BTo-X-contaminated gas stream with a biotrickling filter inoculated with microbes bound to a wheat bran/red wood powder/diatomaceous earth carrier, Bioresour. Technol. 101 (2010) 8067–8073. doi:10.1016/j.biortech.2010.05.096.

[11] R. Lebrero, R. Ángeles, R. Pérez, R. Muñoz, Toluene biodegradation in an algal-bacterial airlift photobioreactor: Influence of the biomass concentration and of the presence of an organic phase, J. Environ. Manage. 183 (2016) 585–593. doi:10.1016/j.jenvman.2016.09.016.

[12] M. Schiavon, M. Ragazzi, E.C. Rada, V. Torretta, Air pollution control through biotrickling filters: a review considering operational aspects and expected performance, Crit. Rev. Biotechnol. 36 (2016) 1143–1155. doi:10.3109/07388551.2015.1100586.

[13] S. Malakar, P. Das Saha, D. Baskaran, R. Rajamanickam, Comparative study of biofiltration

process for treatment of VOCs emission from petroleum refinery wastewater—A review, Environ. Technol. Innov. 8 (2017) 441–461. doi:10.1016/j.eti.2017.09.007.

[14] R. Lebrero, J.M. Estrada, R. Muñoz, G. Quijano, Toluene mass transfer characterization in a biotrickling filter, Biochem. Eng. J. 60 (2012) 44–49. doi:10.1016/j.bej.2011.09.017.

[15] A. Klindworth, E. Pruesse, T. Schweer, J. Peplies, C. Quast, M. Horn, F.O. Glöckner, Evaluation of general 16S ribosomal RNA gene PCR primers for classical and next-generation sequencing-based diversity studies, Nucleic Acids Res. (2013). doi:10.1093/nar/gks808.

[16] R. Schmieder, R. Edwards, Quality control and preprocessing of metagenomic datasets, Bioinformatics. (2011). doi:10.1093/bioinformatics/btr026.

[17] J.G. Caporaso, J. Kuczynski, J. Stombaugh, K. Bittinger, F.D. Bushman, E.K. Costello, N. Fierer, A.G. Pẽa, J.K. Goodrich, J.I. Gordon, G.A. Huttley, S.T. Kelley, D. Knights, J.E. Koenig, R.E. Ley, C.A. Lozupone, D. McDonald, B.D. Muegge, M. Pirrung, J. Reeder, J.R. Sevinsky, P.J. Turnbaugh, W.A. Walters, J. Widmann, T. Yatsunenko, J. Zaneveld, R. Knight, QIIME allows analysis of high-throughput community sequencing data, Nat. Methods. (2010). doi:10.1038/nmeth.f.303.

[18] B.J. Callahan, P.J. McMurdie, M.J. Rosen, A.W. Han, A.J.A. Johnson, S.P. Holmes, DADA2: High-resolution sample inference from Illumina amplicon data, Nat. Methods. (2016). doi:10.1038/nmeth.3869.

[19] C. Quast, E. Pruesse, P. Yilmaz, J. Gerken, T. Schweer, P. Yarza, J. Peplies, F.O. Glöckner, The SILVA ribosomal RNA gene database project: Improved data processing and web-based tools, Nucleic Acids Res. (2013). doi:10.1093/nar/gks1219.

[20] H.W. J. Oksanen, F.G. Blanchet, M. Friendly, R. Kindt, P. Legendre, D. McGlinn, P.R. Minchin, R.B. O'Hara, G.L. Simpson, P. Solymos, M.H.H. Stevens, E. Szoecs, https://cran.r-project.org/web/packages/vegan/index.html, Vegan Community Ecol. Packag. 2.4-4. (2017). https://cran.r-project.org/web/packages/vegan/index.html (accessed November 12, 2018).

[21] B.D. Ondov, N.H. Bergman, A.M. Phillippy, Interactive metagenomic visualization in a Web browser, BMC Bioinformatics. (2011). doi:10.1186/1471-2105-12-385.

[22] M.H. El-Naas, J.A. Acio, A.E. El Telib, Aerobic biodegradation of BTEX: Progresses and Prospects, J. Environ. Chem. Eng. 2 (2014) 1104–1122. doi:10.1016/j.jece.2014.04.009.

[23] D.E.G. Trigueros, A.N. Módenes, A.D. Kroumov, F.R. Espinoza-Quiñones, Modeling of biodegradation process of BTEX compounds: Kinetic parameters estimation by using Particle Swarm Global Optimizer, Process Biochem. 45 (2010) 1355–1361. doi:10.1016/j.procbio.2010.05.007.

[24] H.H. Cox, T.T. Nguyen, M.A. Deshusses, Elimination of toluene vapors in biotrickling filters: performance and carbon balances, in: Proc. Annu. Meet. Exhib. Air Waste Manag. Assoc. June, 1998: pp. 14–18.

[25] J. Song, K.A. Kinney, Microbial response and elimination capacity in biofilters subjected to high toluene loadings, Appl. Microbiol. Biotechnol. 68 (2005) 554–559. doi:10.1007/s00253-005-1956-8.

[26] F.C. Rubio, F.G.A. Fern&#xfffd;ndez, J.A.S. P&#xfffd;rez, F.G. Camacho, E.M. Grima, Prediction of

dissolved oxygen and carbon dioxide concentration profiles in tubular photobioreactors for microalgal culture, Biotechnol. Bioeng. 62 (1999) 71–86. doi:10.1002/(SICI)1097-0290(19990105)62:1<71::AID-BIT9>3.0.CO;2-T.

[27] S. Bordel, R. Muñoz, L.F. Diaz, S. Villaverde, Predicting the Accumulation of Harmful Metabolic Byproducts During the Treatment of VOC Emissions in Suspended Growth Bioreactors, Environ. Sci. Technol. 41 (2007) 5875–5881. doi:10.1021/es070365k.

[28] L. Xu, P.J. Weathers, X.-R. Xiong, C.-Z. Liu, Microalgal bioreactors: Challenges and opportunities, Eng. Life Sci. 9 (2009) 178–189. doi:10.1002/elsc.200800111.

[29] M.B. Leddy, D.W. Phipps, H.F. Ridgway, Catabolite-mediated mutations in alternate toluene degradative pathways in Pseudomonas putida., J. Bacteriol. 177 (1995) 4713–4720.

[30] S. Bordel, R. Muñoz, L.F. Díaz, S. Villaverde, New insights on toluene biodegradation by Pseudomonas putida F1: influence of pollutant concentration and excreted metabolites, Appl. Microbiol. Biotechnol. 74 (2007) 857–866. doi:10.1007/s00253-006-0724-8.

[31] S.J. Haig, C. Quince, R.L. Davies, C.C. Dorea, G. Collins, The relationship between microbial community evenness and function in slow sand filters, MBio. 6 (2015) e00729-15. doi:10.1128/mBio.00729-15.

[32] L. Wittebolle, M. Marzorati, L. Clement, A. Balloi, D. Daffonchio, P. De Vos, K. Heylen, W. Verstraete, N. Boon, Initial community evenness favours functionality under selective stress., Nature. 458 (2009) 623–626. doi:10.1038/nature07840.

[33] J.M. Estrada, E. Rodríguez, G. Quijano, R. Muñoz, Influence of gaseous VOC concentration on the diversity and biodegradation performance of microbial communities, Bioprocess Biosyst. Eng. 35 (2012) 1477–1488. doi:10.1007/s00449-012-0737-x.

[34] P. Juteau, R. Larocque, D. Rho, a LeDuy, Analysis of the relative abundance of different types of bacteria capable of toluene degradation in a compost biofilter., Appl. Microbiol. Biotechnol. 52 (1999) 863–868.

[35] D.H. Parks, M. Chuvochina, D.W. Waite, C. Rinke, A. Skarshewski, P.-A. Chaumeil, P. Hugenholtz, A standardized bacterial taxonomy based on genome phylogeny substantially revises the tree of life, Nat. Biotechnol. 36 (2018). doi:10.1038/nbt.4229.

[36] G. Zwart, B.C. Crump, M.P. Kamst-van Agterveld, F. Hagen, S.K. Han, Typical freshwater bacteria: An analysis of available 16S rRNA gene sequences from plankton of lakes and rivers, Aquat. Microb. Ecol. 28 (2002) 141–155. doi:10.3354/ame028141.

[37] V. Lünsmann, U. Kappelmeyer, R. Benndorf, P.M. Martinez-Lavanchy, A. Taubert, L. Adrian, M. Duarte, D.H. Pieper, M. von Bergen, J.A. Müller, H.J. Heipieper, N. Jehmlich, In situprotein-SIP highlights Burkholderiaceae as key players degrading toluene by para ring hydroxylation in a constructed wetland model, Environ. Microbiol. 18 (2016) 1176–1186. doi:10.1111/1462-2920.13133.

[38] P.M. Martínez-Lavanchy, Z. Chen, V. Lünsmann, V. Marin-Cevada, R. Vilchez-Vargas, D.H. Pieper, N. Reiche, U. Kappelmeyer, V. Imparato, H. Junca, I. Nijenhuis, J.A. Müller, P. Kuschk, H.J. Heipieper, Microbial toluene removal in hypoxic model constructed wetlands occurs predominantly via the ring monooxygenation pathway, Appl. Environ. Microbiol. 81 (2015) 6241–6252. doi:10.1128/AEM.01822-15.

[39] W.M. Chen, L. Moulin, C. Bontemps, P. Vandamme, G. Béna, C. Boivin-Masson, Legume symbiotic nitrogen fixation by β-Proteobacteria is widespread in nature, J. Bacteriol. 185 (2003) 7266–7272. doi:10.1128/JB.185.24.7266-7272.2003.

[40] A. Sessitsch, T. Coenye, A. V. Sturz, P. Vandamme, E.A. Barka, J.F. Salles, J.D. Van Elsas, D. Faure, B. Reiter, B.R. Glick, G. Wang-Pruski, J. Nowak, Burkholderia phytofirmans sp. nov., a novel plant-associated bacterium with plant-beneficial properties, Int. J. Syst. Evol. Microbiol. 55 (2005) 1187–1192. doi:10.1099/ijs.0.63149-0.

[41] D.H. Cho, R. Ramanan, J. Heo, J. Lee, B.H. Kim, H.M. Oh, H.S. Kim, Enhancing microalgal biomass productivity by engineering a microalgal-bacterial community, Bioresour. Technol. 175 (2015) 578–585. doi:10.1016/j.biortech.2014.10.159.

[42] V. Lünsmann, U. Kappelmeyer, A. Taubert, I. Nijenhuis, M. Von Bergen, H.J. Heipieper, J.A. Müller, N. Jehmlich, Aerobic toluene degraders in the rhizosphere of a constructed wetland model show diurnal polyhydroxyalkanoate metabolism, Appl. Environ. Microbiol. 82 (2016) 4126–4132. doi:10.1128/AEM.00493-16.

[43] I. Krohn-Molt, M. Alawi, K.U. Förstner, A. Wiegandt, L. Burkhardt, D. Indenbirken, M. Thieß, A. Grundhoff, J. Kehr, A. Tholey, W.R. Streit, Insights into Microalga and bacteria interactions of selected phycosphere biofilms using metagenomic, transcriptomic, and proteomic approaches, Front. Microbiol. 8 (2017) 1941. doi:10.3389/fmicb.2017.01941.

[44] C. Sambles, K. Moore, T.M. Lux, K. Jones, G.R. Littlejohn, J.D. Gouveia, S.J. Aves, D.J. Studholme, R. Lee, J. Love, Metagenomic analysis of the complex microbial consortium associated with cultures of the oil-rich alga Botryococcus braunii, Microbiologyopen. 6 (2017) e00482. doi:10.1002/mbo3.482.

[45] A. Taylor-Brown, L. Vaughan, G. Greub, P. Timms, A. Polkinghorne, Twenty years of research into Chlamydia-like organisms: A revolution in our understanding of the biology and pathogenicity of members of the phylum Chlamydiae, Pathog. Dis. 73 (2015) 1–15. doi:10.1093/femspd/ftu009.

[46] C.M. Palmer, A COMPOSITE RATING OF ALGAE TOLERATING ORGANIC POLLUTION, J. Phycol. (1969). doi:10.1111/j.1529-8817.1969.tb02581.x.

Figure 1

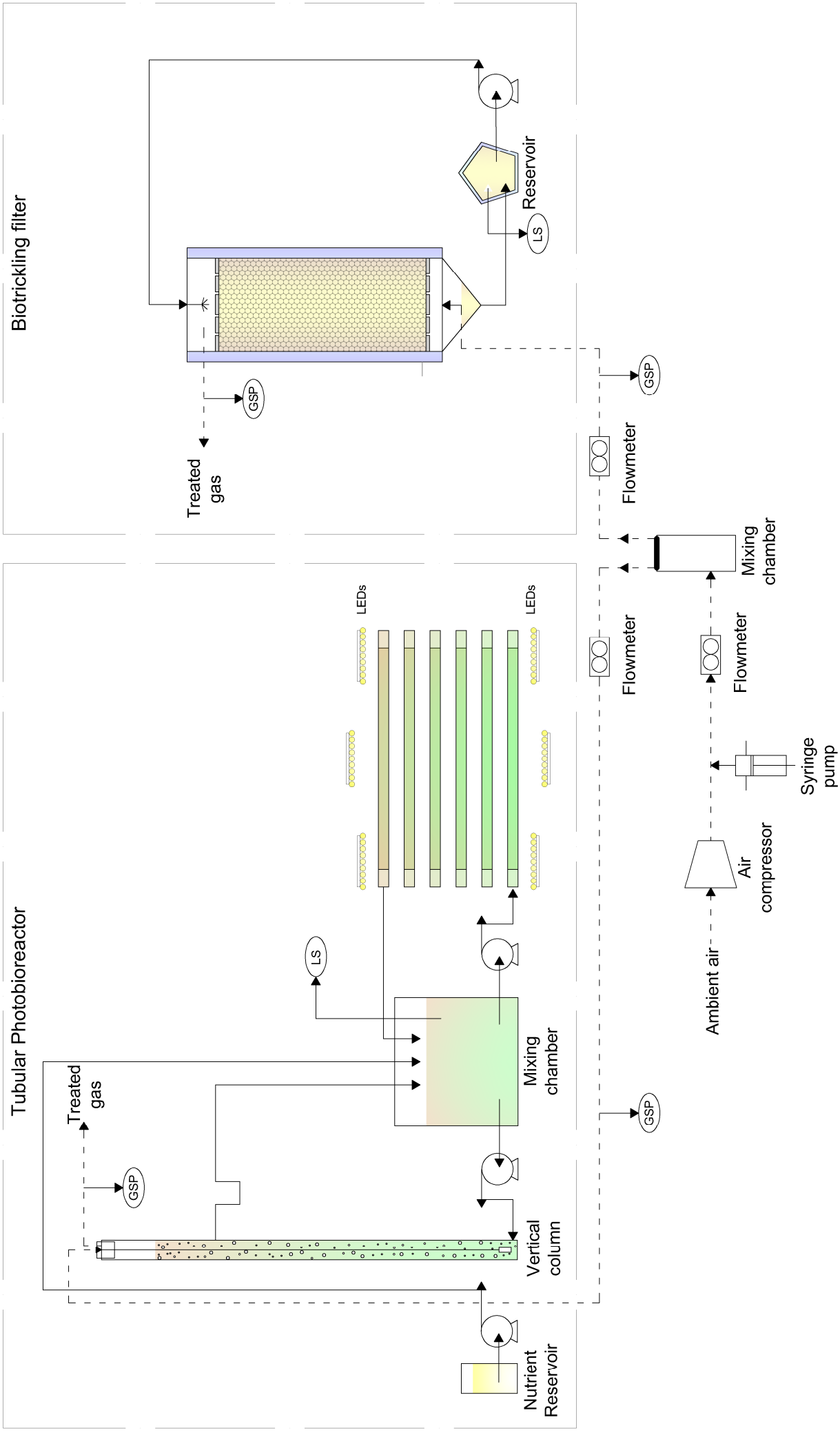
Biotrickling filter
Reservoir
LS
GSP
Treated gas
Flowmeter
Mixing chamber
Flowmeter
Flowmeter
Syringe pump
Air compressor
Ambient air
Tubular Photobioreactor
LEDs
LEDs
LS
Mixing chamber
Treated gas
GSP
GSP
Vertical column
Nutrient Reservoir

Figure 2

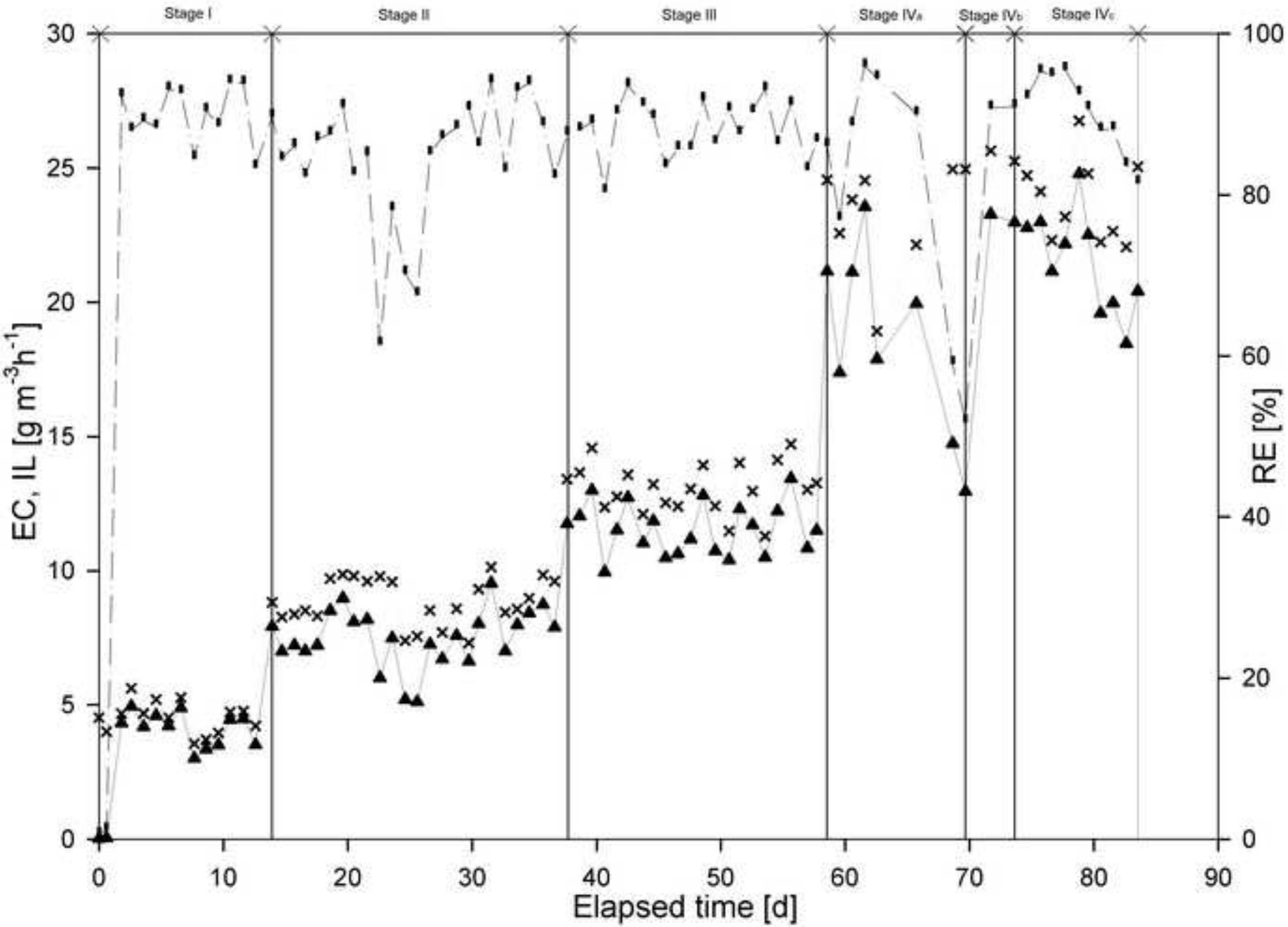
Stage I
Stage II
Stage III
Stage IVA
Stage IVB
Stage IVC
EC, IL [g m-3h-1]
RE [%]
Elapsed time [d]
0
5
10
15
20
25
30
0
20
40
60
80
100
0
10
20
30
40
50
60
70
80
90

Figure 3

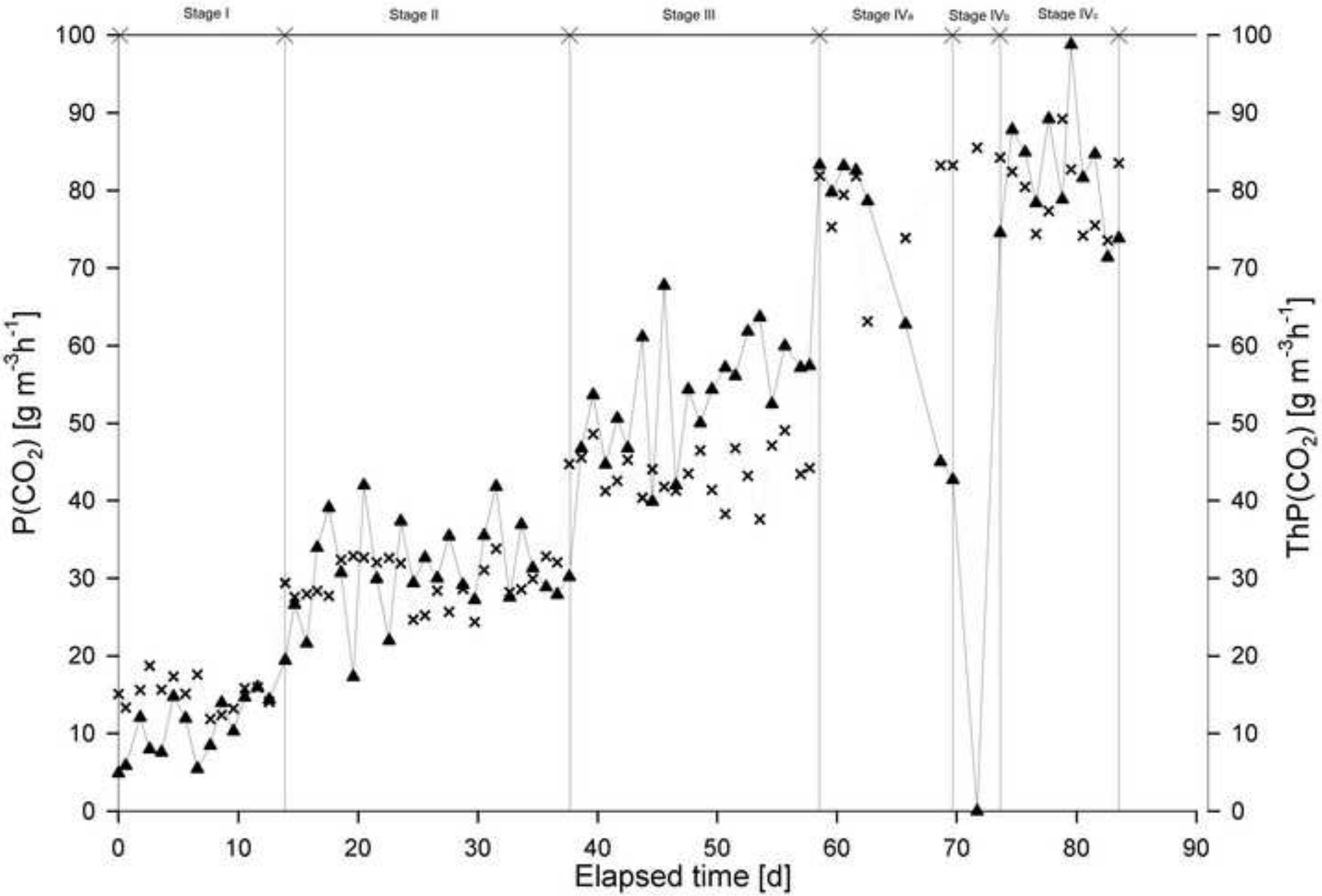
Stage I
Stage II
Stage III
Stage IVa
Stage IVb
Stage IVc
P(CO2) [g m-3h-1]
ThP(CO2) [g m-3h-1]
Elapsed time [d]
0
10
20
30
40
50
60
70
80
90
100

Figure 4

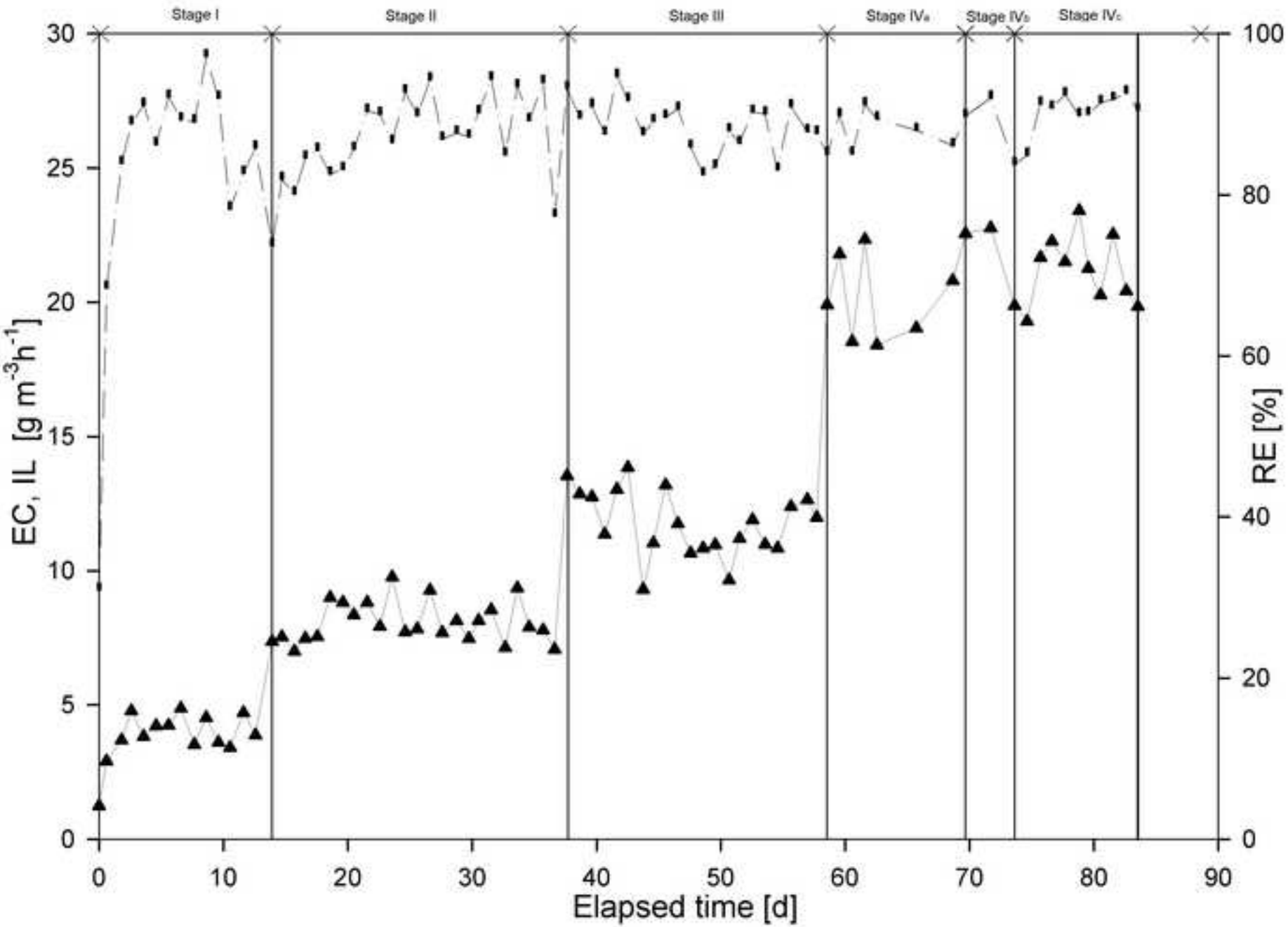
Stage I
Stage II
Stage III
Stage IVa
Stage IVb
Stage IVc
EC, IL [g m-3h-1]
RE [%]
Elapsed time [d]
0
5
10
15
20
25
30
0
20
40
60
80
100
0
10
20
30
40
50
60
70
80
90

Figure 5

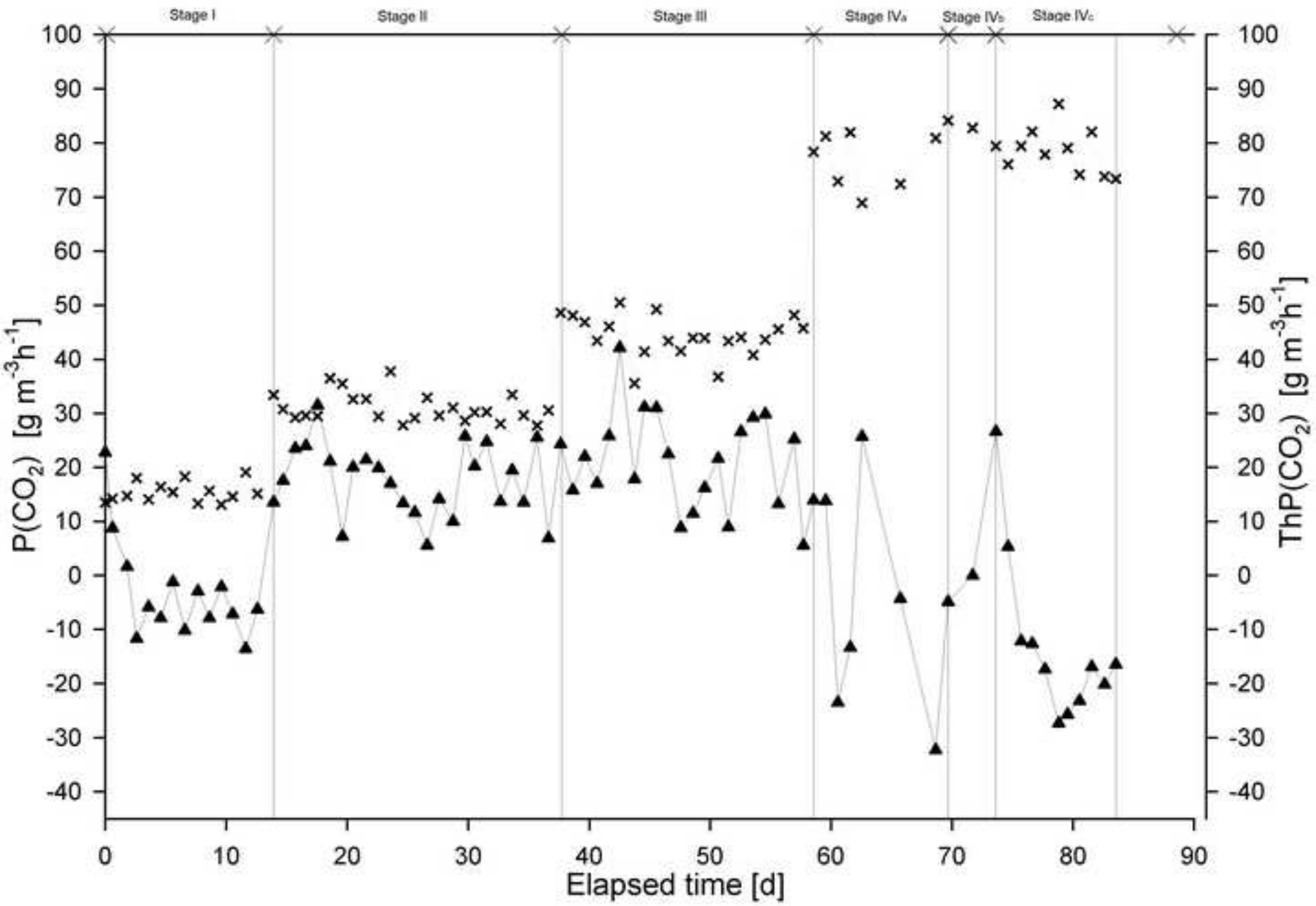
Stage I
Stage II
Stage III
Stage IVA
Stage IVB
Stage IVC
P(CO2) [g m-3h-1]
ThP(CO2) [g m-3h-1]
Elapsed time [d]
100
90
80
70
60
50
40
30
20
10
0
-10
-20
-30
-40
0
10
20
30
40
50
60
70
80
90

Figure 6

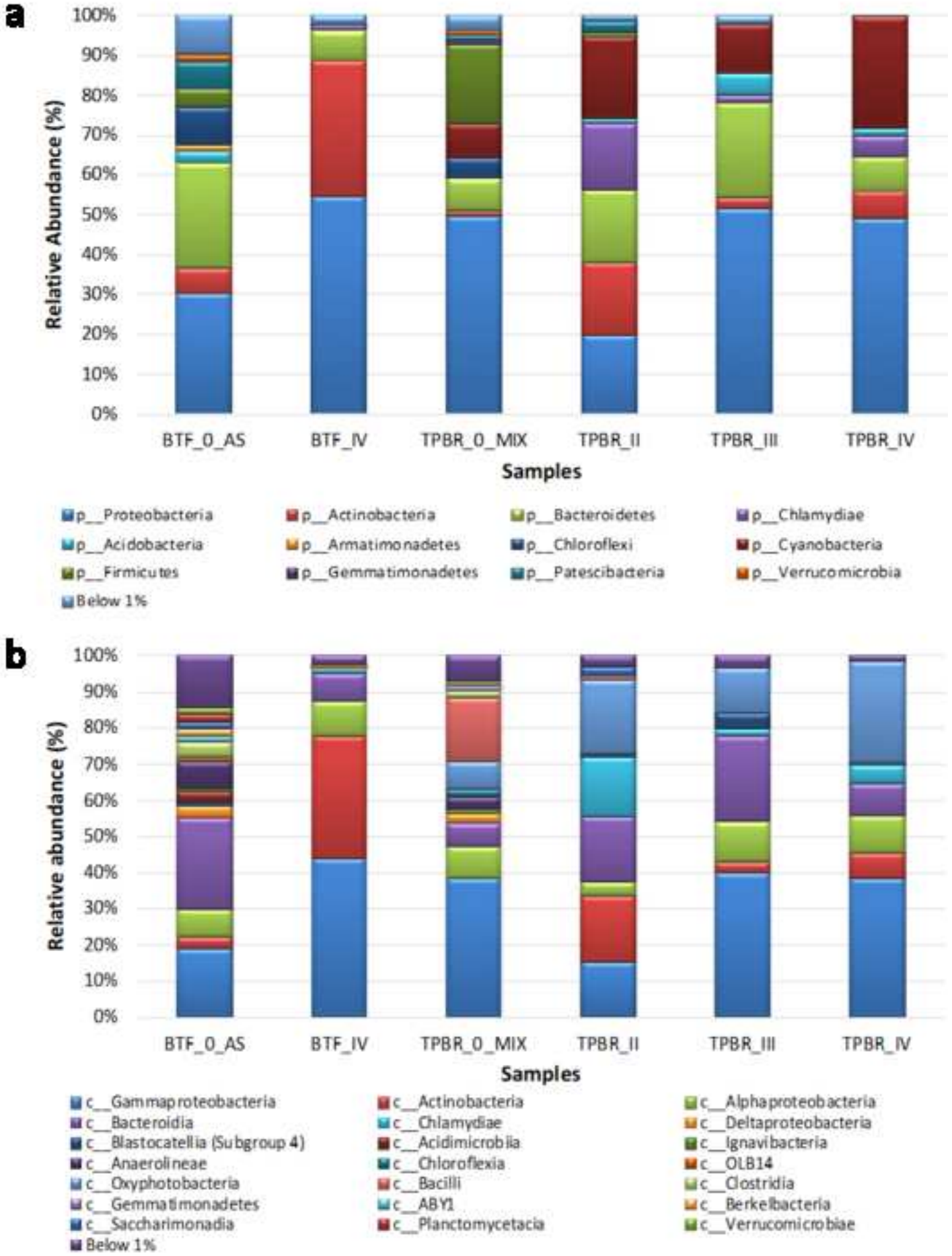
a
100%
90%
80%
70%
60%
50%
40%
30%
20%
10%
0%
Relative Abundance (%)
BTF_0_AS
BTF_IV
TPBR_0_MIX
TPBR_II
TPBR_III
TPBR_IV
Samples
p__Proteobacteria
p__Actinobacteria
p__Bacteroidetes
p__Chlamydiae
p__Acidobacteria
p__Armatimonadetes
p__Chloroflexi
p__Cyanobacteria
p__Firmicutes
p__Gemmatimonadetes
p__Patescibacteria
p__Verrucomicrobia
Below 1%
b
100%
90%
80%
70%
60%
50%
40%
30%
20%
10%
0%
Relative abundance (%)
BTF_0_AS
BTF_IV
TPBR_0_MIX
TPBR_II
TPBR_III
TPBR_IV
Samples
c__Gammaproteobacteria
c__Actinobacteria
c__Alphaproteobacteria
c__Bacteroidia
c__Chlamydiae
c__Deltaproteobacteria
c__Blastocatellia (Subgroup 4)
c__Acidimicrobiia
c__Ignavibacteria
c__Anaerolineae
c__Chloroflexia
c__OLB14
c__Oxyphotobacteria
c__Bacilli
c__Clostridia
c__Gemmatimonadetes
c__ABY1
c__Berkelbacteria
c__Saccharimonadia
c__Planctomycetacia
c__Verrucomicrobiae
Below 1%

Figure 7

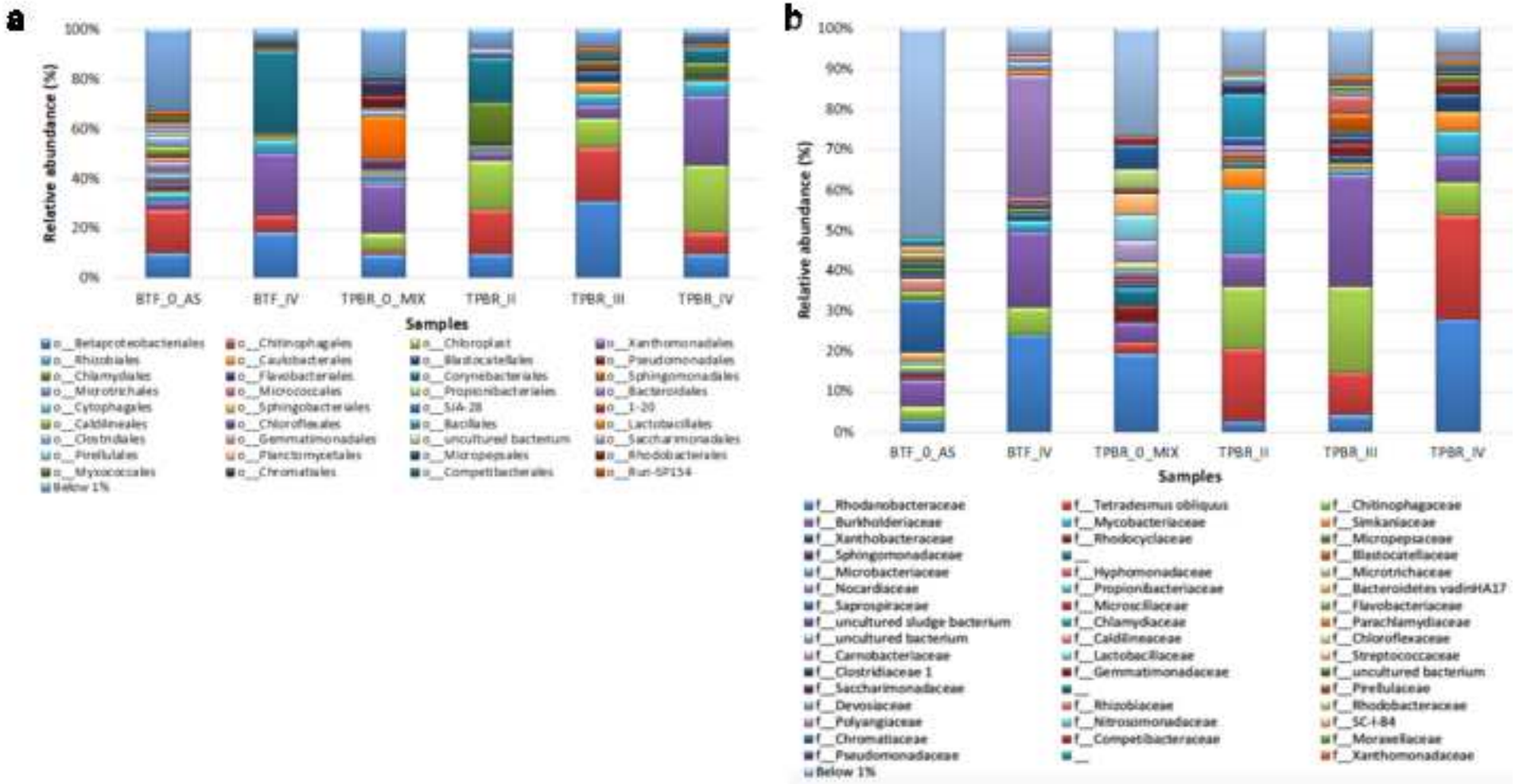
a
100%
80%
60%
40%
20%
0%
Relative abundance (%)
BTF_O_AS
BTF_IV
TPBR_O_MIX
TPBR_II
TPBR_III
TPBR_IV
Samples
o__Betaproteobacteriales
o__Rhizobiales
o__Chlamydiales
o__Microtrichales
o__Cytophagales
o__Caldilineales
o__Clostridiales
o__Pirellulales
o__Myxococcales
Below 1%
o__Chitinophagales
o__Caulobacterales
o__Flavobacteriales
o__Micrococcales
o__Sphingobacteriales
o__Chloroflexales
o__Gemmatimonadales
o__Planctomycetales
o__Chromatiales
o__Chloroplast
o__Blastocatellales
o__Corynebacteriales
o__Propionibacteriales
o__SJA-28
o__Bacillales
o__uncultured bacterium
o__Micropepsales
o__Competibacteriales
o__Xanthomonadales
o__Pseudomonadales
o__Sphingomonadales
o__Bacteroidales
o__1-20
o__Lactobacillales
o__Saccharimonadales
o__Rhodobacterales
o__Run-SP154
b
100%
90%
80%
70%
60%
50%
40%
30%
20%
10%
0%
Relative abundance (%)
BTF_O_AS
BTF_IV
TPBR_O_MIX
TPBR_II
TPBR_III
TPBR_IV
Samples
f__Rhodanobacteraceae
f__Burkholderiaceae
f__Xanthobacteraceae
f__Sphingomonadaceae
f__Microbacteriaceae
f__Nocardiaceae
f__Saprospiraceae
f__uncultured sludge bacterium
f__uncultured bacterium
f__Carnobacteriaceae
f__Clostridiaceae 1
f__Saccharimonadaceae
f__Devosiaceae
f__Polyangiaceae
f__Chromatiaceae
f__Pseudomonadaceae
Below 1%
f__Tetradesmus obliquus
f__Mycobacteriaceae
f__Rhodocyclaceae
f__
f__Hyphomonadaceae
f__Propionibacteriaceae
f__Microscillaceae
f__Chlamydiaceae
f__Caldilineaceae
f__Lactobacillaceae
f__Gemmatimonadaceae
f__
f__Rhizobiaceae
f__Nitrosomonadaceae
f__Competibacteraceae
f__
f__Chitinophagaceae
f__Simkaniaceae
f__Micropepsaceae
f__Blastocatellaceae
f__Microtrichaceae
f__Bacteroidetes vadinHA17
f__Flavobacteriaceae
f__Parachlamydiaceae
f__Chloroflexaceae
f__Streptococcaceae
f__uncultured bacterium
f__Prelulaceae
f__Rhodobacteraceae
f__SC-I-84
f__Moraxellaceae
f__Xanthomonadaceae